Photon Gated Transport at the Glass Nanopore Electrode

4 **AUTHORS**, INCLUDING:

Ilya Zharov
University of Utah

77 PUBLICATIONS **1,484** CITATIONS

Photon Gated Transport at the Glass Nanopore Electrode

Gangli Wang, Andrew K. Bohaty, Ilya Zharov,* and Henry S. White*

Contribution from the Department of Chemistry, University of Utah, 315 South 1400 East, Salt Lake City, Utah 84112

Received June 16, 2006; E-mail: zharov@chem.utah.edu; white@chem.utah.edu

Abstract: The interior surface of the glass nanopore electrode was modified with spiropyran moieties to impart photochemical control of molecular transport through the pore orifice (15−90 nm radius). In low ionic strength acetonitrile solutions, diffusion of a positively charged species ($Fe(bpy)_3^{2+}$) is electrostatically blocked with ∼100% efficiency by UV light-induced conversion of the neutral surface-bound spiropyran to its protonated merocyanine form (MEH^+). Transport through the pore orifice is restored by either irradiation of the electrode with visible light to convert MEH^+ back to spiropyran or addition of a sufficient quantity of supporting electrolyte to screen the electrostatic field associated with MEH^+. The transport of neutral redox species through spiropyran-modified glass nanopores is not affected by light, allowing photoselective transport of redox molecules to the electrode surface based on charge discrimination. The glass nanopore electrode can also be employed as a photochemical trap, by UV light conversion of surface-bound spriropyran to MEH^+, preventing $Fe(bpy)_3^{2+}$ initially in the pore from diffusing through the orifice.

Introduction

We wish to report the chemical surface modification of glass nanopore electrodes in a fashion that leads to a transport-controlled response that can be photochemically switched between "on" and "off" states. Our general strategy is based on integrating molecular transport within nanopores responsive to chemical and physical stimuli,[1−14] with highly sensitive electroanalytical methods for measuring redox species in nanoscale domains. Integration of controlled nanopore transport with electrochemical methods provides a general strategy of fabricating highly sensitive and selective electroanalytical sensors and other devices.

The glass nanopore electrode, Figure 1, is a Pt microdisk electrode embedded at the bottom of a conical pore made in glass, with the circular orifice of the pore having nanometer dimensions currently in the range between 5 and 100 nm. Redox-active molecules diffuse and migrate through the orifice connecting the bulk solution and pore interior. The deep cone-shaped pore possesses an important transport characteristic: the steady-state flux of molecules into the pore is limited by the resistive restriction at the pore orifice and is independent of other geometrical parameters of the pore. We have recently reported a quantitative study of this unique feature, important in understanding transport through nanometer-scale orifices.[15]

In the current report, we describe the chemical modification of the interior pore walls of glass nanopore electrodes, possessing orifices with radii ranging from 15 to 90 nm, with spiropyran moieties. As shown in Scheme 1, spiropyran, either dissolved in solution or attached to a surface, can be reversibly transformed between neutral and positively charged states by irradiation with light of different wavelengths.[16,17] Specifically, spiropyran (SP) is converted from the neutral form (**1a**) to zwitterionic (ME) or cationic merocyanine (MEH^+) forms (**1b/1c**) upon irradiation with UV light, a process that is reversed upon irradiation with visible light. The phototransformation of surface-bound **1a** and **1b/1c** provides a means to selectively gate the flux of redox molecules through the orifice, based on

(1) Ito, T.; Sun, L.; Crooks, R. M. *Anal. Chem.* **2003**, *75*, 2399.
(2) Ito, T.; Sun, L.; Henriquez, R. R.; Crooks, R. M. *Acc. Chem. Res.* **2004**, *37*, 937.
(3) Hinds, B. J.; Chopra, N.; Rantell, T.; Andrews, R.; Gavalas, V.; Bachas, L. G. *Science* **2004**, *303*, 62.
(4) (a) Kasianowicz, J. J.; Brandin, E.; Branton, D.; Deamer, D. W. *Proc. Natl. Acad. Sci. U.S.A.* **1996**, *93*, 13770. (b) Bayley, H.; Cremer, P. S. *Nature* **2001**, *413*, 226. (c) Gu, L.-Q.; Braha, O.; Conlan, S.; Cheley, S.; Bayley, H. *Nature* **1999**, *398*, 686.
(5) Meller, A. *J. Phys.: Condens. Matter* **2003**, *15*, R581.
(6) (a) Fologea, D.; Gershow, M.; Ledden, B.; McNabb, D. S.; Golovchenko, J. A.; Li, J. *Nano Lett.* **2005**, *5*, 1905. (b) Fologea, D.; Gershow, M.; Uplinger, J.; Thomas, B.; McNabb, D. S.; Li, J. *Nano Lett.* **2005**, *5*, 1734. (c) Chen, P.; Gu, J.; Brandin, E.; Kin, Y.-R.; Wang, Q.; Branton, D. *Nano Lett.* **2004**, *4*, 2293. (d) Storm, A. J.; Chen, J. H.; Ling, X. S.; Zandbergen, H. W.; Dekker, C. *Nat. Mater.* **2003**, *2*, 537.
(7) (a) Jirage, K. B.; Hulteen, J. C.; Martin, C. R. *Science* **1997**, *278*, 655. (b) Harrell, C. C.; Lee, S. B.; Martin, C. R. *Anal. Chem.* **2003**, *75*, 6861.
(8) (a) Harrell, C. C.; Kohli, P.; Siwy, Z.; Martin, C. R. *J. Am. Chem. Soc.* **2004**, *126*, 15646. (b) Heins, E. A.; Siwy, Z. S.; Baker, L. A.; Martin, C. R. *Nano Lett.* **2005**, *5*, 1824. (c) Siwy, Z.; Heins, E.; Harrell, C. C.; Kohli, P.; Martin, C. R. *J. Am. Chem. Soc.* **2004**, *126*, 10850.
(9) Lee, S. B.; Martin, C. R. *Anal. Chem.* **2001**, *73*, 768.
(10) Fan, R.; Karnik, R.; Yue, M.; Li, D.; Majumdar, A.; Yang, P. *Nano Lett.* **2005**, *5*, 1633.
(11) (a) Daiguji, H.; Yang, P.; Majumdar, A. *Nano Lett.* **2004**, *4*, 137. (b) Karnik, R.; Fan, R.; Yue, M.; Li, D.; Yang, P.; Majumdar, A. *Nano Lett.* **2005**, *5*, 943.
(12) Newton, M. R.; Bohaty, A. K.; White, H. S.; Zharov, I. *J. Am. Chem. Soc.* **2005**, *127*, 7268.
(13) Newton, M. R.; Bohaty, A. K.; Zhang, Y.; White, H. S.; Zharov, I. *Langmuir* **2006**, *22*, 4429.
(14) Cichelli, J.; Zharov, I. *J. Am. Chem. Soc.* **2006**, *128*, 8130.
(15) (a) Zhang, B.; Zhang, Y.; White, H. S. *Anal. Chem.* **2004**, *76*, 6229. (b) Zhang, B.; Zhang, Y.; White, H. S. *Anal. Chem.* **2006**, *78*, 477. (c) Zhang, Y.; Zhang, B.; White, H. S. *J. Phys. Chem. B* **2006**, *110*, 1768.
(16) Bertelson, R. C. Spiropyrans. In *Organic Photochromic and Thermochromic Compounds*; Crano, J. C., Guglielmetti, R. J., Eds.; Plenum Publishing Corp.: New York, NY, 1999; p 11.
(17) Sheng, Y.; Leszczynski, J.; Garcia, A. A.; Rosario, R.; Gust, D.; Springer, J. *J. Phys. Chem. B* **2004**, *108*, 16233.
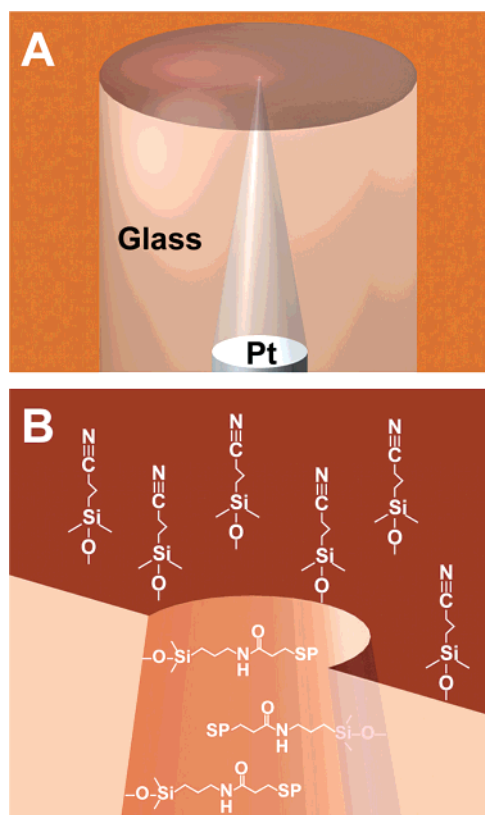
Figure 1. (A) Schematic representation of a glass nanopore electrode used in obtaining experimental results reported in this Article (15-nm-orifice radius, 0.9-μm-base, 2.8 μm depth, and 0.75-mm-radius glass shroud, drawn to scale except for the glass shroud). (B) Interior and exterior surfaces of the glass nanopore modified, respectively, with spiropyran and cyanopropyl groups.

Scheme 1
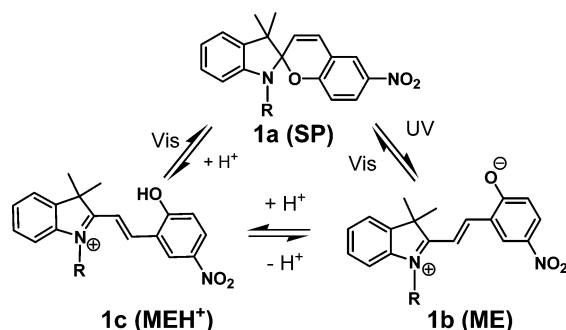
the charge of the redox molecule. In relation to this approach, control of surface properties has been demonstrated for spiropyran-modified inorganic surfaces,[18] including switchable wettability of flat,[19] porous,[20] and polymer surfaces.[21,22] Recently, a protein channel has been modified with a single spiropyran molecule, and its reversible opening and closing has been

achieved by UV and visible light irradiation.[23] Photoisomerization of azobenzene in a nanoporous membrane has also been used to control the mass transport at an indium tin oxide electrode.[24] A previous report from our laboratories demonstrated that it is possible to modify the interior nanopore surface with amine functionalities, allowing the surface charge and redox molecule flux to be controlled by adjusting the pH.[25] The present paper extends this surface chemistry inside the glass nanopore to a more complex system and demonstrates that flux through glass nanopore can be controlled by an external physical stimulus.

Experimental Section

General. Bis(cyclopentadienyl)iron (ferrocene, Fc, Alfa Aesar, 100%), trifluoroacetic acid (TFA, Acros, 99%), 3-cyanopropyldimethyl-chlorosilane ($Cl(Me)_2Si(CH_2)_3CN$), and 3-aminopropyl-dimethylethoxy-silane ($EtO(Me)_2Si(CH_2)_3NH_2$) (Gelest, Inc.) were used as received. Tris(bipyridine)iron(II) perfluorate ($Fe(bpy)_3(PF_6)_2$) was synthesized according to literature procedures.[26] Acetonitrile (CH_3CN, HPLC grade, J. T. Baker) was stored over 3-Å molecular sieves. Spiropyran *N*-hydroxysuccinimidyl ester (**2**) was synthesized following literature procedures.[27,28] UV−vis spectra of acetonitrile solutions containing spiropyran-modified silica spheres (137-nm radius) were recorded using an Ocean Optics USB2000 spectrometer. A 366-nm UV hand-held lamp (UVP Inc. 115 V, 0.16 A) and two incandescent lamps (collimated 30 W and uncollimated 75 W) were used as UV and visible photon sources, respectively. Glass nanopore electrodes were positioned 5−10 cm from the lamps during irradiation to prevent an increase in temperature of the electrode.

Fabrication and Surface Modification of Glass Nanopore Electrodes. Preparation of the spiropyran-modified electrodes closely follows a recently detailed procedure for covalent attachment of a propylamine silane monolayer to the interior surface of glass nanopore electrodes.[25] Briefly, the preparation involves the following steps: (1) a 25-μm diameter Pt wire (Alfa-Aesan, 99.95%) is electrochemically etched to produce a sharp tip with ∼10 nm radius of curvature; (2) the sharpened Pt tip is sealed in a Corning 8161 Pb glass capillary (Warner Instruments Inc., i.d. = 1.10 mm; o.d. = 1.50 mm); (3) the capillary is polished until a Pt nanodisk is exposed; (4) the electrode is thoroughly cleaned by sonication in H_2O, EtOH, CH_3CN, and H_2O, soaking in 1 M HNO_3 for 10 min, followed by rinsing in H_2O and CH_3CN; (5) the electrode is immersed overnight in an CH_3CN solution containing ∼2% v/v $Cl(Me)_2Si(CH_2)_3CN$, resulting in covalent attachment of cyano-propyl silane to the exterior glass surface; (6) the exposed Pt disk is etched in a 15% $CaCl_2$ solution (pH ≈ 5.5) with 5 V ac voltage applied between the Pt nanoelectrode and a Pt wire counter to produce a truncated cone-shaped nanopore in glass, the bottom of the pore defined by a Pt microdisk electrode; (7) the interior glass surface is modified in an CH_3CN solution containing ∼2% v/v $EtO(Me)_2Si(CH_2)_3NH_2$ using the above procedure; and (8) NHS ester **2** is attached to the surface-attached −NH_2 groups by soaking the amine-modified nanopore electrode in 0.01 M CH_3CN solution of **2** for 48 h. The final electrode structure is shown in Figure 1. The ability to chemically modify the exterior and interior pore surfaces with siloxanes containing different functional groups was previously established by selective covalent

(18) Vlassiouk, I.; Park, C.-D.; Vail, S. A.; Gust, D.; Smirnov, S. *Nano Lett.* **2006**, *6*, 1013.
(19) Rosario, R.; Gust, D.; Hayes, M.; Jahnke, F.; Springer, J.; Garcia, A. A. *Langmuir* **2002**, *18*, 8062.
(20) Bunker, B. C.; Kim, B. I.; Houston, J. E.; Rosario, R.; Garcia, A. A.; Hayes, M.; Gust, D.; Picraux, S. T. *Nano Lett.* **2003**, *3*, 1723.
(21) (a) Chung, D. J.; Ito, Y.; Imanishi, Y. *J. Appl. Polym. Sci.* **1994**, *51*, 2026. (b) Park, Y. S.; Ito, Y.; Imanishi, Y. *J. Macromolecules* **1998**, *31*, 2606.
(22) Athanassiou, A.; Lygeraki, M. I.; Pisignano, D.; Lakiotaki, K.; Varda, M.; Mele, E.; Fotakis, C.; Cingolani, R.; Anastasiadis, S. H. *Langmuir* **2006**, *22*, 2329.

(23) Kocer, A.; Walko, M.; Meijberg, W.; Feringa, B. L. *Science* **2005**, *309*, 755.
(24) Liu, N.; Dunphy, D. R.; Atanassov, P.; Bunge, S. D.; Chen, Z.; Lopez, G. P.; Boyle, T. J.; Brinker, C. J. *Nano Lett.* **2004**, *4*, 551.
(25) Wang, G.; Zhang, B.; Wayment, J. R.; Harris, J. M.; White, H. S. *J. Am. Chem. Soc.* **2006**, *128*, 7679.
(26) Sarkar, D.; Subbarao, P. V.; Begum, G.; Ramakrishna, K. *J. Colloid Interface Sci.* **2005**, *288*, 591.
(27) Fissi, A.; Pieroni, O.; Ruggeri, G.; Ciardelli, F. *Macromolecules* **1995**, *28*, 302.
(28) Zhang, P.; Meng, J.; Li, X.; Matsuura, T.; Wang, Y. *J. Heterocycl. Chem.* **2002**, *39*, 179.

Scheme 2
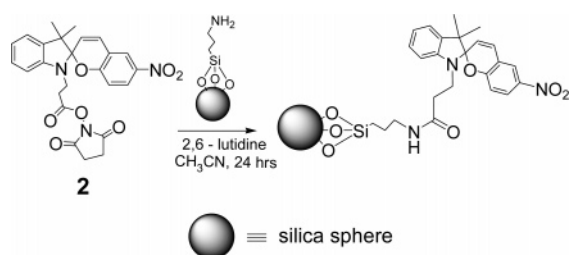
attachment of a highly fluorescent probe molecule, 5-(and-6)-carboxy-tetramethylrhodamine succinimidyl ester, to $-NH_2$ sites on the interior glass surface followed by fluorescence micrscopy to demonstrate the spatially localized attachment of the probe molecule.[25]

The radius of the nanopore orifice (*a*) is estimated by measuring the voltammetric limiting current at the Pt nanodisk, prior to etching the Pt in the $CaCl_2$ solution. The diffusion-limited voltammetric current (i_d) for the oxidation of 5 mM ferrocene (Fc) in CH_3CN is given by $i_d = 4nFDC*a$, where *n* is the number of electrons transferred, *F* is Faraday's constant, and *D* is the diffusion coefficient of Fc (2.4×10^{-5} cm^2/s).[29] Using slightly larger electrodes ($a = 75-100$ nm), we have shown that the electrochemical measurement yields values that are within 20% of the values determined by scanning electron[15b] and atomic force microscopies.[30] The smallest electrodes used in this study have not yet been successfully imaged. Thus, all radii reported here are "apparent" radii, based on the electrochemical response. Nanopore depths were measured from the cone angle of the etched wire and the dependence of peak current on scan rate in fast scan voltammetric, as previously detailed.[15]

Electrochemical Measurements. Voltammetric data were obtained using a Cypress model EI-400 bipotentiostat interfaced to a PC through an AT-MIO16E-10 or a PCI 6251 data acquisition board (National Instruments). Voltammetric data were recorded using in-house virtual instrumentation written in LabView (National Instrument). A one-compartment, two-electrode cell with either a Ag wire or a Ag/AgNO$_3$ (CH_3CN, 0.01 M AgNO$_3$, 0.1 M TBAP) reference/auxiliary electrode was employed with the cell and preamplifier in a Faraday cage. Other details of the electrochemical measurements have been previously described.[25]

Results and Discussion

Reversible electrostatic photogating of redox molecule transport though the orifice of the glass nanopore can by achieved by covalent attachment of spiropyran moieties to the interior pore surface. The photochromic behavior of surface-bound spiropyran moieties has been extensively studied in aqueous solution,[19] organic solutions,[31] and at the solid−air interface,[20] but not at the glass/CH_3CN interface. Thus, to determine if surface-bound spiropyran moieties undergo transformations described in Scheme 1 in the presence of CH_3CN, we initially modified the surface of 137-nm radius silica spheres with spiropyran derivative **2** (Scheme 2) and recorded the UV spectra of the resulting modified spheres in CH_3CN in the presence of trifluoroacetic acid (TFA) before and after irradiation with UV and visible light. Silica spheres were selected for the model studies because they provide surface properties similar to those of the glass nanopore and allow direct spectroscopic observation of surface-bound spiropyran transformations in CH_3CN. Upon irradiation of spiropyran-modified silica spheres with UV light (366 nm for 15 min), the colorless colloidal solution became
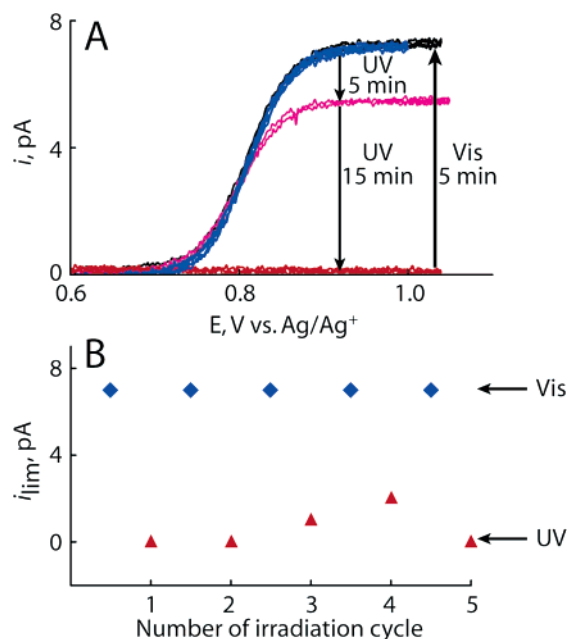
(29) Kuwana, T.; Bubitz, D. E.; Hoh, G. *J. Am. Chem. Soc.* **1960**, *82*, 5811.
(30) Zhang, B.; White, H. S. Unpublished results, University of Utah, 2006.
(31) Raymo, F. M.; Giordani, S. *J. Org. Chem.* **2003**, *68*, 4158.

Figure 2. (A) Voltammetric response of a 15-nm-radius, 2.8-μm-deep spiropyran-modified glass nanopore electrode in a CH_3CN solution containing 5 mM Fe(bpy)$_3$(PF$_6$)$_2$ and 20 μM TFA. Blue, before irradiation; magenta, after irradiation with UV light for 5 min; red, after additional irradiation with UV light for 15 min; black, after irradiation with visible light for 5 min. (B) The magnitude of the voltammetric limiting current during five on−off irradiation cycles with UV and visible light.

pink and a new absorption centered at 557 nm appeared in the spectrum. This absorption band is characteristic of zwitterionic merocyanine (ME) in CH_3CN ($\lambda_{max} = 570$).[32] The surface-bound ME was converted back to spiropyran (SP) by irradiation with a visible light source for 40 min or by simply exposing the colloidal solution to ambient light. When the experiment was repeated in the presence of either 1 or 10 equiv of TFA, UV irradiation resulted in a yellow colloidal solution with an absorption maximum at 450 nm, characteristic of the protonated merocyanine (MEH$^+$) in CH_3CN ($\lambda_{max} = 410$ nm).[32] Surface-bound MEH$^+$ could also be converted back to the closed form by irradiating the silica spheres solution with visible light (40 min).

Modified glass nanopores (Figure 1) were prepared by covalent attachment of cyanopropyl groups to the exterior surface (creating an inert polar surface to prevent specific interaction of permeants), followed by etching the Pt wire to produce a nanopore. The interior surface of the glass pore was then treated with EtO(Me)$_2$Si(CH$_2$)$_3$NH$_2$ to generate a $-NH_2$ terminated surface,[25] followed by treatment with **2** (analogous to Scheme 2) to introduce photoactive spiropyran moieties on the glass surface (Figure 1B).

The influence of UV and visible irradiation on the steady-state voltammetric response of the spiropyran-modified glass nanopore electrodes was investigated in CH_3CN solutions containing 5 mM Fe(bpy)$_3{}^{2+}$ and 20 μM TFA. A freshly prepared spiropyran-modified electrode with a 15-nm radius orifice, in the dark, displays a steady-state sigmoidal-shaped voltammogram for oxidation of Fe(bpy)$_3{}^{2+}$ centered at $E_{1/2} \approx$ 0.80 V vs Ag/AgNO$_3$ (Figure 2). The magnitude of the voltammetric current plateau reflects the reaction rate-limiting

(32) Reference 31 reports slightly different absorption maxima for ME ($\kappa_{max} = 563$) and MEH$^+$ ($\kappa_{max} = 401$ nm).

diffusion of the $Fe(bpy)_3^{2+}$ through the pore orifice, a general characteristic of transport in conical pores.[15] Irradiation of this and other similarly prepared electrodes (see additional examples in the Supporting Information) with 366 nm light for 5−15 min resulted in reduction of the faradaic current for $Fe(bpy)_3^{2+}$ oxidation to background levels. The duration of irradiation required for complete transport blockage varied from electrode to electrode and is likely due to either the differences in surface coverage or the differences in alignment of the nanopore orifice relative to the light source. Glass nanopore electrodes irradiated with the UV light in CH_3CN containing only TFA showed similar blockage of $Fe(bpy)_3^{2+}$ transport when placed in solution containing both TFA and $Fe(bpy)_3^{2+}$. The voltammetric current can be restored by exposure to visible light for 5 min, shown in Figure 2A. We attribute the decrease in current upon exposure of the electrode to UV light to electrostatic repulsion of $Fe(bpy)_3^{2+}$ by photogenerated MEH^+, and the restoration of the voltammetric signal in visible light to photoregeneration of spiropyran.

The reversibility of transport gating at the glass nanopore was investigated using five different electrodes with orifice radii ranging from 15 to 90 nm. Figure 2B shows the voltammetric limiting current for $Fe(bpy)_3^{2+}$ oxidation during five orifice open/closed cycles. Typically, relatively good reproducibility was observed for 5−10 cycles, followed by a gradual decrease in the blocking efficiency upon irradiation with UV light. We speculate that the loss of photoresponse is due to the photo-degradation of spiropyran moieties.[33] Glass nanopore electrodes with smaller orifice radii (15−40 nm) generally showed more effective blocking upon UV light irradiation as compared to electrodes with larger nanopores (60−90 nm radii).

In control experiments, irradiation of unmodified glass nanopore electrodes, Figure 3A, and spiropyran-modified glass micropore electrodes with very large orifice radii, for example, 2 μm (Figure 3B), did not show any effect on the voltammetric response in $Fe(bpy)_3^{2+}$ solutions. The absence of a photoresponse at electrodes with larger pore radii is anticipated, as the electric field associated with the surface-bound MEH^+ decays over a very short distance that is defined by the solution Debye length, κ^{-1}. Typically, the extension of the electric field from the surface is taken as $\sim 3\ \kappa^{-1}$.[34] In a 5 mM $Fe(bpy)_3(PF_6)_2$ solution, κ^{-1} is of the order of 5 nm and the surface charge associated with MEH^+ generates an electrostatic field that extends on the order of 15 nm, significantly smaller than the 2 μm orifice radius of the electrode employed in the control experiment presented in Figure 3B. Thus, the vast majority of the pore interior is field free, allowing $Fe(bpy)_3^{2+}$ to diffuse freely regardless of the charge state of the SP moiety. Conversely, the electric field essentially fills the entire solution volume at the orifice of a 15 nm glass nanopore electrode, resulting in strong repulsive interactions between the MEH^+ and $Fe(bpy)_3^{2+}$.

We observed significant current blockage upon UV irradiation at modified glass nanopore electrodes with orifice radii as large as 90 nm (see Supporting Information). In this case, the Debye
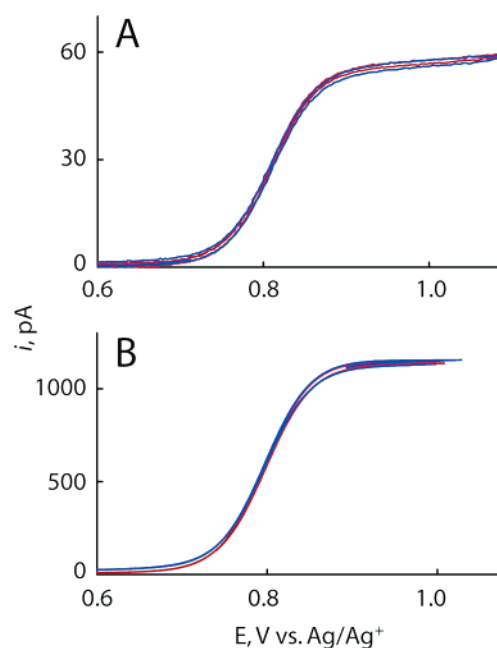

Figure 3. Voltammetric response of (A) a 90-nm-radius unmodified glass nanopore electrode, and (B) a 2-μm-radius spiropyran-modified glass micropore electrode with the interior surface in a CH_3CN solution containing 5 mM $Fe(bpy)_3(PF_6)_2$ and 20 μM TFA after irradiation with UV (blue) or visible (red) light for 5−15 min.

length is likely to be too short for the electrical field to effectively fill the entire pore orifice. This observed blocking in large pores might be explained by the following two factors. First, some uncertainty exists in the size and shape of the pore orifice, which is based on electrochemical measurement of the radius of an assumed disk-shaped electrode. In addition, the magnitude of the electrostatic field depends on the surface density of photogenerated MEH^+. Thus, the variability in the surface coverage of SP is expected to yield electrodes that block the steady-state flux of $Fe(bpy)_3^{2+}$ to different degrees.

Spiropyran moieties are introduced into glass nanopores using the amine-modified surface. Thus, if any residual amino groups are still present on the surface, they might become protonated by TFA and affect the transport of positively charged species through the nanopore orifice.[25] However, we expect that the phenolate groups in zwitterionic spiropyran moieties would be protonated prior to protonation of the less basic amino groups. In a control experiment, the transport of $Fe(bpy)_3^{2+}$ through the orifice of amine-modified nanopore electrodes (without SP attachment) in CH_3CN was not blocked by addition of 20 μM TFA to protonate the surface amines. Blocking was observed using 1−10 mM TFA, indicating that these groups are indeed less basic than phenolate.[35]

To confirm that nanopore blocking is due to the electrostatic repulsion between MEH^+ and $Fe(bpy)_3^{2+}$, experiments were performed in which a strong electrolyte, tetrabutylammonium perchlorate (TBAP), was added to the solution following UV irradiation. TBAP fully dissociates in CH_3CN and is thus anticipated to screen the surface charge resulting from photogeneration of MEH^+. Figure 4A shows the results of an experiment in which the current that was blocked after UV irradiation was immediately and nearly completely restored

(33) (a) Irie, M.; Tamaki, T.; Seki, T.; Hibino, J. *Photochromic Spiropyrans*; Bunshin: Tokyo, 1993. (b) Tagaya, H.; Nagaoka, T.; Kuwahara, T.; Karasu, M.; Kadokawa, J.; Chiba, K. *Microporous Mesoporous Mater.* **1998**, *21*, 395.
(34) Probstein, R. F. *Physiochemical Hydrodynamics*; Butterworths: Boston, 1989.

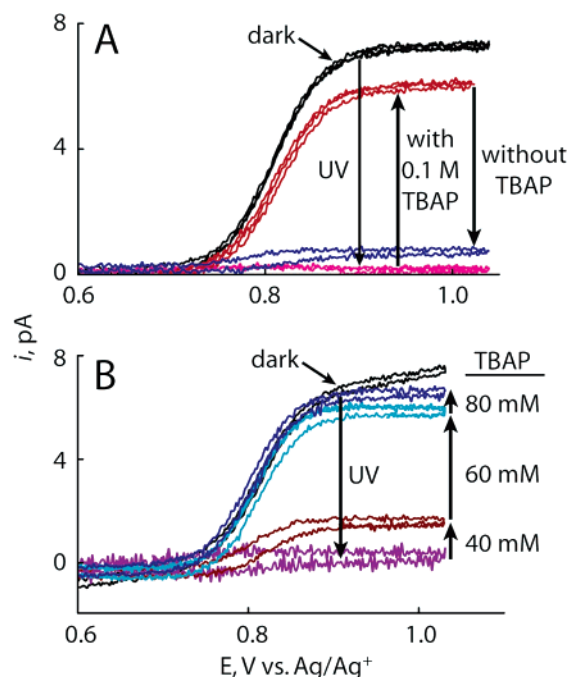(35) Electrostatic blockage in aqueous solutions at amine-modified glass nanopore electrodes occurred at pH 4.[25]

Figure 5. Voltammetric response of a spiropyran-modified 44-nm-radius, 1.8-μm-deep spiropyran-modified glass nanopore electrode in a CH$_3$CN solution containing 1 mM ferrocene, 5 mM Fe(bpy)$_3$(PF$_6$)$_2$, and 20 μM TFA. The black curve corresponds to the initial electrode response recorded in the dark. The red and blue curves correspond to, respectively, the electrode response after 15 min irradiation with UV light and then 15 min irradiation with visible light.

Figure 4. Influence of the electrostatic screening of the surface charge resulting from photogeneration of MEH$^+$. (A) Voltammetric response of a 15-nm-radius, 1.8-μm-deep spiropyran-modified glass nanopore electrode in a CH$_3$CN solution containing 5 mM Fe(bpy)$_3$(PF$_6$)$_2$ and 20 μM TFA before (black curve) and after (pink curve) irradiation with UV light for 15 min. Following irradiation, the electrode was placed in the dark in a CH$_3$-CN solution containing 5 mM Fe(bpy)$_3$(PF$_6$)$_2$, 20 μM TFA, and 0.1 M TBAP solutions (red curve), and then placed back into the original solution (blue curve). (B) Influence of incremental increases of supporting electrolyte concentration on electrostatic gating following irradiation with UV light (transition between black and purple curves).

when the electrode was placed, without exposure to visible light, in a 5 mM Fe(bpy)$_3$(PF$_6$)$_2$/20 μM TFA solution containing 0.1 M TBAP. Placing the electrode back into the solution without TBAP resulted in the original decrease in current resulting from UV photogenerated MEH$^+$.

The concentration of supporting electrolyte required to fully unblock the nanopore orifice, determined by incremental addition of TBAP to the CH$_3$CN solution, was between one and several hundred millimolar, with significant variation between experiments using different nanopore electrodes. Figure 4B shows a representative experiment in which the voltammetric response was recorded as a function of TBAP concentration and the limiting current was restored gradually with increasing supporting electrolyte concentration. The observed variation in the concentration of TBAP required to completely screen the MEH$^+$ surface charge at different electrodes is likely due to differences in the number of surface MEH$^+$ moieties created and differences in the orifice radii.

Charge selectivity of electrostatic gating at the spiropyran-modified nanopore was demonstrated using a CH$_3$CN solution containing a neutral redox species, ferrocene (Fc), and positively charged Fe(bpy)$_3$$^{2+}$. The voltammetric response at a freshly modified 44-nm-radius glass nanopore electrode, prior to being irradiated with UV light, displayed steady-state voltammetric responses for both redox species (Figure 5). As before, the magnitude of the voltammetric limiting current corresponds to the rate-limiting diffusion of Fc and Fe(bpy)$_3$$^{2+}$ through the nanopore orifice. After the glass nanopore electrode was irradiated by UV light for 15 min in a separate CH$_3$CN solution
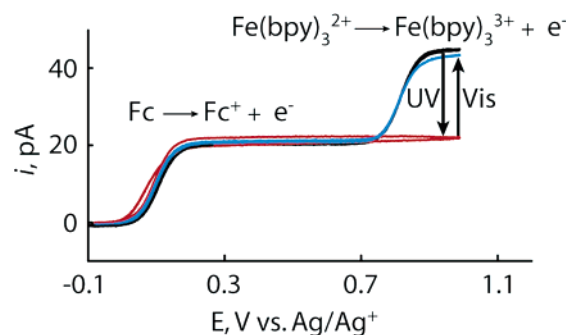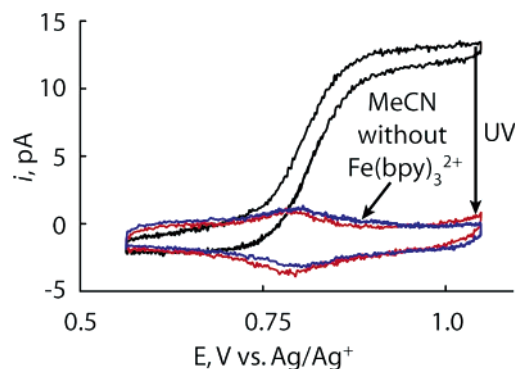
Figure 6. Electrostatic trapping of Fe(bpy)$_3$$^{2+}$ inside a 30-nm-radius, 6.2-μm-deep nanopore electrode. The black and red curves correspond to the spiropyran-modified glass nanopore electrode in a CH$_3$CN solution containing 5 mM Fe(bpy)$_3$(PF$_6$)$_2$ and 20 μM TFA before and after UV irradiation, respectively. The blue curve was recorded in CH$_3$CN containing 20 μM TFA without Fe(bpy)$_3$(PF$_6$)$_2$.

containing 20 μM TFA and placed back into the redox solution, the voltammetric response corresponding to oxidation of Fe(bpy)$_3$$^{2+}$ disappeared, while that for Fc oxidation remained essentially unchanged. Exposure of the electrode to visible light restored the current for Fe(bpy)$_3$$^{2+}$ oxidation without affecting the response for Fc. (An unexplained caveat of this experiment is that direct UV irradiation of the electrode in the mixed redox solution appears to cause adsorption of Fc on the nanopore electrode surface, leading to poorly reproducible behavior.)

Finally, we note that the spiropyran-modified glass nanopore electrodes can also be used to trap very small quantities of molecules using external light sources, based on the principles described above. Figure 6 shows the response at a spiropyran-modified nanopore electrode (30-nm-radius orifice, 6.2-μm-deep nanopore) in a CH$_3$CN solution containing 5 mM Fe(bpy)$_3$$^{2+}$ and 20 μM TFA. After UV irradiation, the steady-state limiting current disappears and a symmetrical peak-shaped voltammogram appears. The peak-shaped voltammetric response arises from the redox molecules trapped inside the pore prior to photogeneration of MEH$^+$ and is reproducibly observed for electrodes containing deep nanopores with small orifice radii. To demonstrate that the Fe(bpy)$_3$$^{2+}$ is electrostatically blocked from diffusing from the pore orifice, the electrode was transferred in the dark to a CH$_3$CN solution containing only 20 μM TFA. An essentially identical voltammetric response was obtained (blue curve) as observed in the Fe(bpy)$_3$$^{2+}$ solution.

In control experiments in which TFA is omitted or in which the electrode is intentionally irradiated with visible light, the peak-shaped voltammetric response is not observed when the electrode is transferred to the CH$_3$CN solution. A detailed investigation of the trapping and release of molecules using glass nanopore electrodes is currently underway.

The voltammetric response of trapped molecules is similar to that of a classic "thin-layer" electrochemical cell comprising a thin rectangular volume bounded by closely spaced parallel electrode and insulating surfaces.[36] Integration of the area under the peak yields an electrical charge corresponding to ~2.6 × 10^7 Fe(bpy)$_3^{2+}$ molecules trapped in the pore following photoclosure of the pore orifice. Based on the conical shape pore volume (6.3 × 10^{-12} cm^3), this value corresponds to an Fe(bpy)$_3^{2+}$ concentration of ~4 mM, in excellent agreement with the 5 mM concentration of Fe(bpy)$_3^{2+}$ inside of the nanopore prior to irradiation.

The appearance of a thin-layer response requires a sufficiently large number of trapped molecules to produce a faradaic current, as these measurements are made close to the limit of detection in slow scan voltammetry. Because the volume of a cone increases as the cube of the cone height, the thin-layer response is not easily observed for very shallow pores (with corresponding small solution volumes). The response in Figure 6 corresponds to a 6.2-μm-deep nanopore electrode containing ~2.6 × 10^7 molecules. Much smaller trapping peaks are observed in the responses shown in Figure 4 and in Figure SI2 of the Supporting Information for, respectively, 2.8- and 1.8-μm-deep glass nanopore electrodes.

(36) (a) Anson, F. C. *Anal. Chem.* **1961**, *33*, 1498. (b) Christensen, C. R.; Anson, F. C. *Anal. Chem.* **1963**, *35*, 205.

Conclusions

Chemical modification of the interior surface of the glass nanopore electrode with spiropyran provides a highly efficient means to gate molecular transport through a nanometer-scale orifice using photons. In essence, the spiropyran-modified nanopore acts as a photoswitch, in which a small number of photons, absorbed by spiropyran moieties in the pore orifice, induce reversible gating of the steady-state flow of charged species through the pore orifice. This finding, as well as results from our previous report, demonstrate that a single pore orifice, synthesized in a mechanically and chemically robust support, that is, glass, can be employed as a molecular gate. The general result is promising in developing stable and relatively simple devices for drug delivery and chemical sensing. Efforts in this laboratory are now directed to understanding the relationship between the photoactivated charge distribution at the orifice and transport rates (e.g., the number of photogenerated charges required for gating), as well as to modification of the pore surface to make gating responsive to specific analytes.

Supporting Information Available: Additional examples of the photoresponse of spiropyran-modified electrodes. This material is available free of charge via the Internet at http://pubs.acs.org.

JA064274J